

Phase Transition of MoS Bilayer Structures

Mohnish Pandey, Pallavi Bothra, and Swapan K. Pati

J. Phys. Chem. C, **Just Accepted Manuscript** • DOI: 10.1021/acs.jpcc.5b10904 • Publication Date (Web): 02 Feb 2016

Downloaded from <http://pubs.acs.org> on February 8, 2016

Just Accepted

“Just Accepted” manuscripts have been peer-reviewed and accepted for publication. They are posted online prior to technical editing, formatting for publication and author proofing. The American Chemical Society provides “Just Accepted” as a free service to the research community to expedite the dissemination of scientific material as soon as possible after acceptance. “Just Accepted” manuscripts appear in full in PDF format accompanied by an HTML abstract. “Just Accepted” manuscripts have been fully peer reviewed, but should not be considered the official version of record. They are accessible to all readers and citable by the Digital Object Identifier (DOI®). “Just Accepted” is an optional service offered to authors. Therefore, the “Just Accepted” Web site may not include all articles that will be published in the journal. After a manuscript is technically edited and formatted, it will be removed from the “Just Accepted” Web site and published as an ASAP article. Note that technical editing may introduce minor changes to the manuscript text and/or graphics which could affect content, and all legal disclaimers and ethical guidelines that apply to the journal pertain. ACS cannot be held responsible for errors or consequences arising from the use of information contained in these “Just Accepted” manuscripts.

Phase Transition of MoS₂ Bilayer Structures

Mohnish Pandey,^{*,†} Pallavi Bothra,[‡] and Swapan K. Pati^{‡,¶}

Center for Atomic-scale Materials Design, Department of Physics, Technical University of Denmark, DK - 2800 Kongens Lyngby, Denmark, New Chemistry Unit, Jawaharlal Nehru Centre for Advanced Scientific Research, Bangalore, India, and Theoretical Sciences Unit, Jawaharlal Nehru Centre for Advanced Scientific Research, Bangalore, India

E-mail: mohpa@fysik.dtu.dk

*To whom correspondence should be addressed

[†]Center for Atomic-scale Materials Design, Department of Physics, Technical University of Denmark, DK - 2800 Kongens Lyngby, Denmark

[‡]New Chemistry Unit, Jawaharlal Nehru Centre for Advanced Scientific Research, Bangalore, India

[¶]Theoretical Sciences Unit, Jawaharlal Nehru Centre for Advanced Scientific Research, Bangalore, India

Abstract

In the present study, using density functional calculations we have investigated a possible mechanism for the structural phase transition of the semiconducting bilayer 2H-MoS₂ via lithiation. The results indicate that the addition of lithium to the bilayer 2H-MoS₂ transforms the bilayer to a heterostructure of the 2H and 1T structures instead of a complete conversion to the 1T bilayer structure. Therefore, we propose that the desired synthesis of the 1T-MoS₂ from the bulk 2H-MoS₂ takes place through the hybrid 2H-1T structure. Our finding gives physical insight to the experimentally described microscopic mechanism of the phase transition in MoS₂ and enrich the atomic scale understanding of the interaction of MoS₂ with the alkali ions and also other transition metal dichalcogenides manifesting similar phase transition.

Keywords: Heterostructure, density functional theory, bilayer, phase transition, lithiation

Introduction

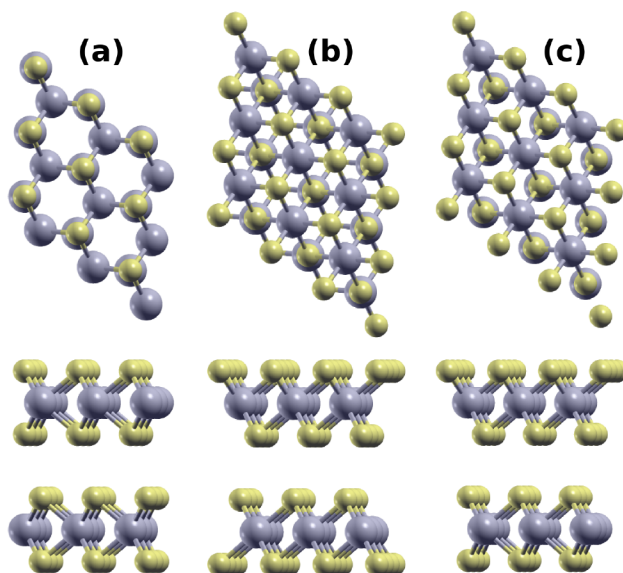
In the past decade low dimensional materials have drawn much attention due to their unique chemical and physical properties in comparison to their bulk counterparts. The dimensionality reduction may lead to zero-dimensional structure like quantum dots, one dimensional-structures like nanotubes or two-dimensional (2D) structures like graphene. The 2D structures have attracted significant attention due to the advent of graphene and other 2D materials like monolayer or few layers of the MoS₂. One of the decisive factor for a significant change in the electronic properties of a few layer and the monolayer structure of the layered compounds like MoS₂ is the interlayer coupling. Although, the coupling is weak but it has dramatic effects on the electronic properties of the layered materials.¹ For example, monolayer MoS₂ is a direct bandgap semiconductor whereas the nature of the bandgap changes from direct to indirect if the number of layers is increased to two or more.² In the recent years, monolayer MoS₂ has been explored for a wide gamut of applications, for example, in flexible transistors and sensors,³⁻⁶ photoluminescence,⁷⁻⁹ batteries¹⁰ and photodetectors.¹¹

1
2
3
4 The naturally occurring bulk structure of the MoS₂ known as ‘2H’ structure has a trigonal
5 prismatic structure.¹² In the monolayer form it has also been synthesized in a different
6 structure known as ‘1T’ structure which has an octahedral symmetry.¹² The undistorted 1T
7 structure is metallic in nature^{8,13,14} whereas it has been found that the 1T-MoS₂ structure
8 shows distortions which gives rise to interesting electronic properties.^{15,16} Recently Qian *et*.
9 *al* have proposed the existence of the Quantum Spin Hall (QSH) effect in the distorted
10 1T-MoS₂ and it has also been explored for hydrogen evolution reaction (HER)..^{12,16} On the
11 other hand, 1T-MoS₂ despite having useful properties does not exist naturally and has to be
12 derived from the 2H-MoS₂.
13
14
15
16
17
18
19
20

21 Different methods have been explored to derive 1T-MoS₂ from the bulk 2H-MoS₂.¹⁷⁻²⁰
22 One of the most widely used method involves the intercalation of alkali metal ions in the
23 interlayer spacing of the multilayer structure. Subsequently, the hydration of the alkali ions
24 increases the distance between the layers thus leading to exfoliation of the 1T-MoS₂.²¹⁻²⁴
25 Unlike mechanical exfoliation to isolated monolayers from the bulk structure, the intercala-
26 tion method can also be used to tune the crystal structure of the MoS₂. For example, tuning
27 the crystal structure of MoS₂ in the intercalation method using lithium as an intercalant
28 involves the inclusion of the lithium to the MoS₂ crystal which changes in *d*-electron count
29 via electron transfer from the valence *s*-orbital of the lithium to the lowest lying unoccupied
30 energy levels of the transition metal center. In order to accommodate the additional charge
31 a local rearrangement of the atomic structure takes place accompanied by the metal-metal
32 bond distortions²⁵ which eventually leads to the transformation of the 2H structure of MoS₂
33 to the 1T structure.
34
35
36
37
38
39
40
41
42
43
44
45
46
47

48 However, despite the large body of work done on the phase transition of the monolayer
49 2H-MoS₂ to 1T structure, we lack a detailed understanding of the phase transition involving
50 multilayers. Since, the synthesis 1T-MoS₂ in the monolayer form takes place by intercalating
51 the bulk 2H-MoS₂, having an understanding of the phase transition in multilayers will give
52 a more realistic picture of the mechanism involved in the synthesis of the monolayer 1T-
53
54
55
56
57
58
59
60

1
2
3
4 MoS₂. Therefore, in the present work we study the phase transition of the bilayer 2H-
5 MoS₂. Our findings suggest that the lithiation process in the bilayer involves a combination
6 of intercalation and adsorption of lithium. Additionally, we find that instead of complete
7 transformation of both the layers of the 2H structure to the 1T structure, the transformation
8 leads to a heterostructure of the 2H and 1T phases. Based on energetics we find that the 1T
9 side of the heterostructure originates from the 2H layer which has adsorbed and intercalated
10 lithium and not from the 2H layer which has only intercalated lithium. Therefore, based on
11 thermodynamic arguments we suggest that the transformation of the 2H-MoS₂ to 1T-MoS₂
12 starts from the surface and permeates to the bulk. 1 (a) shows the top and side view of the
13 2H structure, (b) shows the bilayer of 1T structure and (c) corresponds to a heterostructure
14 of the 2H and 1T phase.
15
16
17
18
19
20
21
22
23
24
25



46
47
48
49
50
51
52
53
54
55
56
57
58
59
60

Figure 1: (a) The top and side view of the bilayer of the 2H structure. (b) Similar as (a) for the 1T structure. (c) The heterostructure comprising of monolayer of each of the 2H and 1T structure.

Computational Methodology

All the calculations have been performed using the density functional theory as implemented in Quantum Espresso.²⁶ Throughout the work the generalized gradient approximation was employed using PW91 functional.²⁷ The ionic cores have been described by the ultrasoft pseudopotentials taken from the publicly available repository of the Quantum Espresso distribution. Brillouin zone sampling was performed with Monkhorst-Pack scheme²⁸ and the k-point grid of $4 \times 4 \times 1$ has been chosen for all the calculations. The wavefunctions were expanded with a plane wave basis set with a kinetic energy cutoff of 30 Ryd. Electronic occupancies were allowed by using an energy smearing of 0.01 Ryd of Marzari-Vanderbilt scheme. The bilayer MoS₂ surfaces in the present study were represented as two-dimensional slabs in a 3D periodic cell with a periodic $2 \times 2 \times 1$ unit cell with 15 Å vacuum to avoid any spurious interactions. Additionally, to account for van der Waals interactions dispersion corrections were employed. We use ‘DFT-D2’ treatment of Grimme, which gives a fairly accurate treatment of London dispersion interactions at relatively low computational cost.²⁹ Structural optimizations were performed until the forces on each atom become less than 10^{-3} eV Å⁻¹. For the calculation of the activation barriers climbing image nudged elastic band method (CI-NEB) was used.³⁰ In order to make sure that the transition takes place via the translation of the sulfur planes as suggested by experiments,³¹ few intermediate images with translated sulfur planes are provided for the NEB calculation.

Results and Discussion

In most of the previous experiments the 2H phase of MoS₂ bulk in powder form has been used as a precursor to obtain the 1T phase. On the other hand, recent theoretical studies on the 2H to 1T transformation has been carried out for monolayers. Phase transition involving only the monolayers will be a plausible route when the 2H precursor itself is in the monolayer form. However, most of the lithiation mediated solution phase synthesis of

1
2
3
4 the 1T structure has been performed with the bulk MoS₂ in the 2H phase. Therefore, it is
5 possible that the synthetic route of the 1T structure with the bulk MoS₂ precursor requires
6 more than one layer of MoS₂. In the current work we explore one such possibility of the
7 phase transition of the 2H to 1T structure in bilayer form via commonly used lithiation
8 process. We emphasize that approximating a multilayer structure by a bilayer structure will
9 not significantly affect the energetics. The effect of hybridization (direct to indirect band gap
10 transition) is already captured in going from the monolayer to bilayer regime. Additionally,
11 the interlayer spacing in the bilayer structure is very close to the interlayer spacing in the
12 bulk. Therefore, approximating a multilayer structure by a bilayer structure is justified for
13 the purpose of the energetics.
14
15
16
17
18
19
20
21
22
23

24 As pointed out earlier, the charging (lithiation) of the 2H phase induces an instability in
25 the structure. Eventually, the instability leads to distortions driving the transition from the
26 semiconducting 2H phase to the metallic 1T phase above a threshold charging i.e. above a
27 certain concentration of lithium. Since the 2H and 1T structure differ from each other by a
28 translation of the sulfur plane as shown in the, therefore, a process which eases the translation
29 will drive the transition. Additionally, apart from favoring the distortion, lithiation also
30 weakens the sulfur-metal bonds thus assisting the translation of the sulfur atoms.
31
32
33
34
35
36
37

38 In the initial stage of Li addition to the 2H-MoS₂, the following reaction takes place
39 $x\text{Li} + \text{MoS}_2 \rightarrow \text{Li}_x\text{MoS}_2$ without any substantial change in the atomic structure. This
40 phenomenon has been demonstrated previously in a high resolution scanning transmission
41 electron microscope (STEM)³¹ imaging where a heterojunction of the 2H and 1T phase has
42 been observed within the intermediate range of x . In the above mentioned experiment,
43 upon gradual addition of Li atom to the host lattice, a critical range of x is reached where
44 the complete phase transition from the 2H to 1T phase is observed. Additionally, it was
45 also observed that excess addition of the Li atoms, i.e. under deep lithiation 1T-LiMoS₂
46 transforms into Li₂S and Mo cluster. Since the whole process depends solely on the Li atom
47 stoichiometry x , it is vital to get the clear understanding of critical concentration of Li that
48
49
50
51
52
53
54
55
56
57
58
59
60

1
2
3
4 stabilizes a particular phase along with a possible mechanism of the phase transition of the
5
6 2H to 1T.

7
8 In order to have a microscopic understanding of the possible mechanism of the lithia-
9
10 tion driven phase transition of the MoS₂ bulk we explore different structures of the MoS₂
11
12 bilayer as a model system. The addition of Li atoms in the bilayer structure may result
13
14 to following possibilities (1) 2H-2H bilayer (2H-2H) (2) 1T-1T bilayer (1T-1T) (3) A het-
15
16 erostructure consist of the 2H and 1T monolayers generating 2H-1T bilayer (2H-1T). These
17
18 possibilities have also been observed in previous experiments^{8,32-34} thus suggesting the tran-
19
20 sition via multilayer structures a plausible route. Using bilayer as a representative system
21
22 for the multilayer structure we assess the thermodynamic stability of the bilayers upon Li
23
24 intercalation/adsorption we calculate the binding energy E_b as,

$$E_b = E^{\text{Li}_x\text{MoS}_2} - xE_{\text{Li}} - E_{\text{MoS}_2} \quad (1)$$

25
26
27
28
29
30
31 where $E^{\text{Li}_x\text{MoS}_2}$, E_{Li} and E_{MoS_2} are the total energies of the lithiated MoS₂, bulk lithium and
32
33 the pure MoS₂ host bilayer respectively and x indicates the number of Li atoms in $E^{\text{Li}_x\text{MoS}_2}$.

34
35 In lithiation of the bilayers, the Li atoms can either be intercalated or adsorbed on
36
37 the surface; hence lithiation in bilayers is different from the monolayer structure where
38
39 the lithium atoms can only be in an adsorbed state. This difference might give rise to
40
41 different energetics in the monolayer and the bilayer structure. Therefore, in order to study
42
43 the thermodynamics of lithiation in the bilayers we systematically adsorb and intercalate
44
45 lithium atoms and choose the configuration with lowest energy. As a result, we find that the
46
47 lithiation proceeds via combination of intercalation and adsorption in the following order;
48
49 intercalation → intercalation → adsorption → intercalation → adsorption. Binding energies
50
51 of Li are found to be negative for all concentrations, however, it is clear from 2 (a) that
52
53 binding of Li is more favourable with 1T-MoS₂ than to 2H-MoS₂. The stronger Li binding
54
55 with the 1T polytype can be justified with the help of crystal field theory.^{35,36} For 2H-MoS₂,
56
57
58
59
60

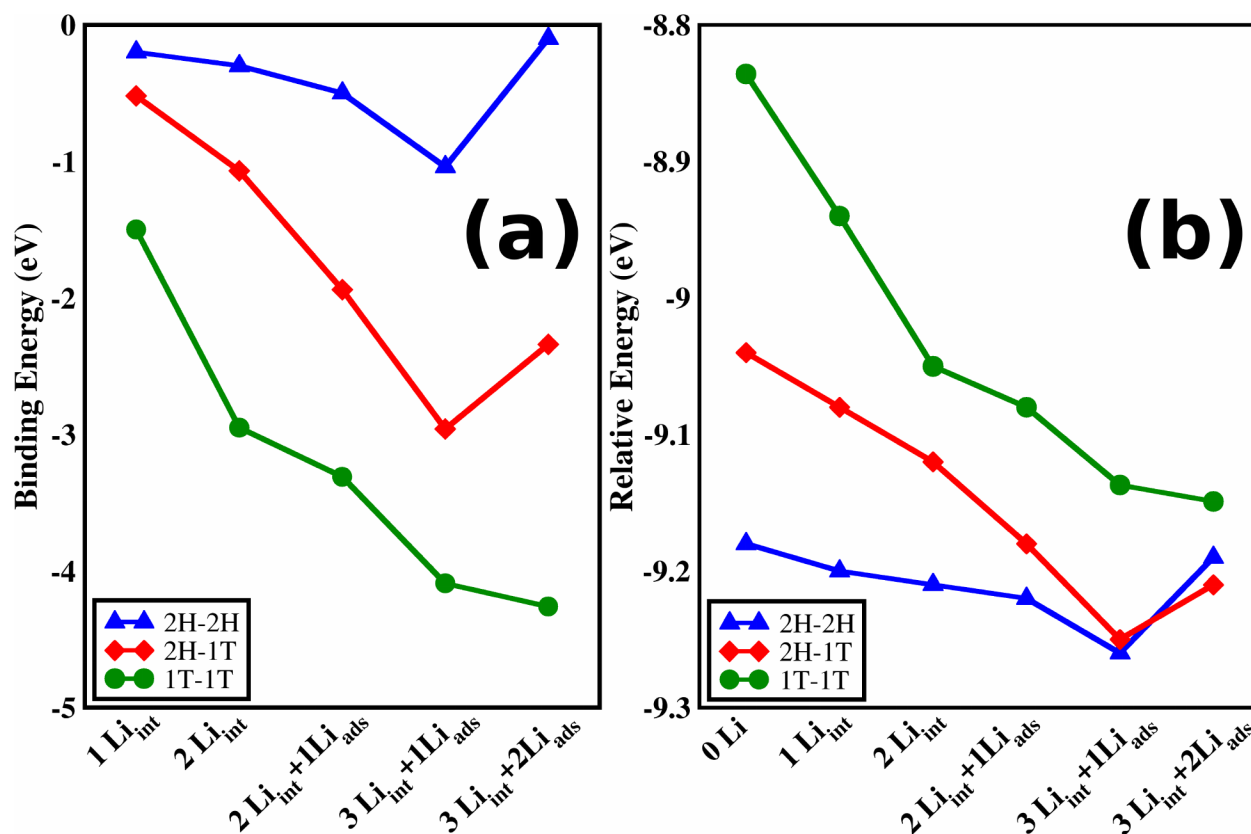


Figure 2: (a) Binding energy per Li atom for 2H-2H, 2H-1T and 1T-1T bilayer of Li_xMoS_2 as a function of Li concentration. Li_{int} and Li_{ads} correspond to intercalated and adsorbed lithium, respectively. (b) Relative energy of 2H-2H, 2H-1T and 1T-1T bilayers as a function of Li concentration.

1
2
3 the lowest energy orbital, Mo $4d_{z^2}$ is fully occupied, hence an electron from donor Li has
4 to take in the higher energy orbitals, $4d_{xy}$ and $4d_{x^2-y^2}$. On the other hand, for the 1T-MoS₂,
5
6 the lowest energy orbitals ($4d_{xy}$, $4d_{yz}$ and $4d_{xz}$) are degenerate and partially occupied; hence,
7
8 readily accommodate the electrons from Li which leads to a larger negative binding energy.
9
10

11 In order to find out the critical concentration of Li atoms which initiates the phase
12 transition of the 2H-2H bilayer, the relative energies of Li incorporated (2H-1T) and (1T-
13 1T) bilayers have been computed with respect to 2H-2H bilayer. The relative energies are
14 shown in 2 (b). As evident from 2 (b), 2H-2H bilayer is the most stable phase over the
15 concentration range of four Li atoms. However, addition of the fifth Li atom makes the
16 2H-1T bilayer more stable than 2H-2H one indicating greater thermodynamic stability of
17 the 2H-1T bilayer. The addition of electron donors (Li) in large concentrations causes a
18 mutation of Mo-*d* orbitals stabilising the octahedral coordination of Mo in 1T phase leading
19 to a junction of two different domain boundaries, 2H and 1T layers.³⁷ The highest energy of
20 1T-1T phase throughout the lithiation process suggests that there is no probable formation
21 of 1T-1T phase as an intermediate during the transition. It can be concluded from the
22 above observations that the transformation of the bulk 2H-MoS₂ to the bulk 1T-MoS₂ is a
23 dynamical process which takes place layer by layer.
24
25
26
27
28
29
30
31
32
33
34
35
36
37

38 Based on the above thermodynamic analyses we explore the kinetics of one possible
39 pathway for the phase transition. The pathway explored involves the gliding of the sulfur
40 plane which breaks the mirror plane symmetry of the 2H monolayer and converts it to a
41 1T monolayer. The suggested route for the phase transition is qualitatively similar to the
42 recent experiments exploring the mechanism of phase transition involves gliding of the sulfur
43 atomic plane which occurs in two stages, namely nucleation of the 1T phase and growth
44 of the 1T phase via migration of the two domain boundaries.³¹ The suggested pathway is
45 shown in the 3. The kinetic barriers are calculated with and without the lithiation and are
46 shown in the 1. The table clearly shows that the lithiation significantly reduces the barrier
47 and it has the minimum value for the 2H-2H \rightarrow 2H-1T transition. Additionally, the final
48
49
50
51
52
53
54
55
56
57
58
59
60

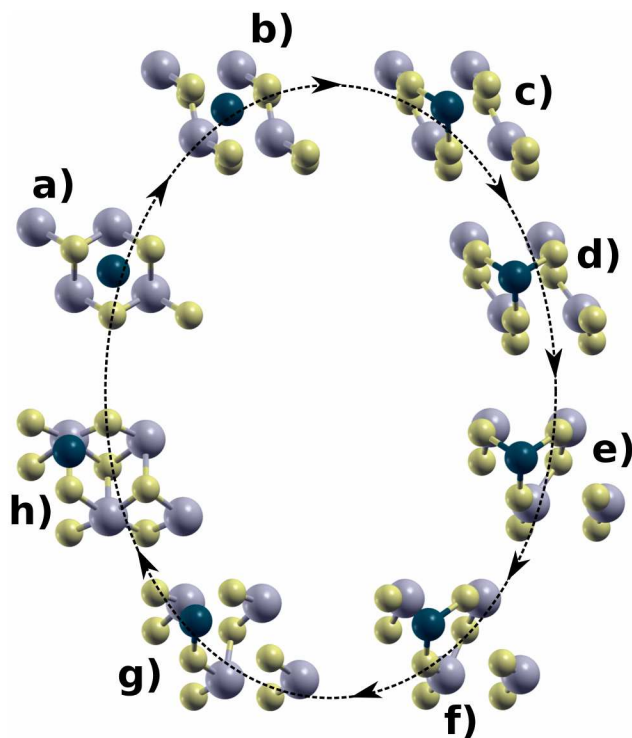


Figure 3: Top view of few steps involved in the proposed pathway for the transition of the 2H structure to the 1T structure via lithiation. (a) represents the starting 2H phase whereas (h) represents end product of the transition i.e. the 1T phase and the remaining sub-figures show intermediate structures. Grey, yellow and dark cyan spheres represent molybdenum, sulfur and lithium atoms respectively.

step being de-lithiation in the process of solution phase synthesis, the back transition of the 2H-1T bilayer is prevented due to significantly large barrier for the transition of the 1T structure to the 2H structure in the absence of lithium.

Table 1: Kinetic barriers for the phase transition. ‘BL’ denotes bilayer whereas ‘ML’ denotes monolayer. All the barriers are in eV

Structure	Lithiation	Barrier (eV)
2H-2H (BL) \rightarrow 2H-1T (BL)	yes	0.70
2H (ML) \rightarrow 1T (ML)	yes	0.95
1T (ML) \rightarrow 2H (ML)	yes	0.43
2H (ML) \rightarrow 1T (ML)	no	1.72
1T (ML) \rightarrow 2H (ML)	no	0.95

Conclusion

In the current study we explore the thermodynamics of lithiation driven transition of the bilayer 2H-MoS₂ to the bilayer of 1T structure and a heterostructure containing the 2H and 1T monolayers. The study of the bilayer is expected to represent the phase transition of the bulk MoS₂. The results show that the lithiation occurs in a combination of intercalation and adsorption thus favoring the transition initiating from the surface layer and permeating to the bulk. Additionally, the calculated kinetic barrier for different pathways indicate that the inclusion of lithium significantly decreases the barrier in all the cases. The agreement of our model systems and results and few recent experiments makes our approach potentially useful for other metal dichalcogenides existing in the 2H and 1T structure and their phase transition. The findings of this study help in identifying possible transition pathways and guides towards the synthesis of the different phases of transition metal dichalcogenides.

Acknowledgments

PB acknowledges the CSIR for a research fellowship. SKP acknowledges research support from the CSIR and DST, Government of India.

References

- (1) Jin, W.; Yeh, P.-C.; Zaki, N.; Zhang, D.; Sadowski, J. T.; Al-Mahboob, A.; van der Zande, A. M.; Chenet, D. A.; Dadap, J. I.; Herman, I. P. et al. Direct Measurement of the Thickness-Dependent Electronic Band Structure of MoS₂ Using Angle-Resolved Photoemission Spectroscopy. *Phys. Rev. Lett.* **2013**, *111*, 106801.
- (2) Lee, H. S.; Min, S.-W.; Chang, Y.-G.; Park, M. K.; Nam, T.; Kim, H.; Kim, J. H.; Ryu, S.; Im, S. MoS₂ Nanosheet Phototransistors with Thickness-Modulated Optical Energy Gap. *Nano Lett.* **2012**, *12*, 3695–3700.
- (3) Yoon, Y.; Ganapathi, K.; Salahuddin, S. How Good Can Monolayer MoS₂ Transistors Be? *Nano Lett.* **2011**, *11*, 3768–3773.
- (4) Li, H.; Yin, Z.; He, Q.; Li, H.; Huang, X.; Lu, G.; Fam, D. W. H.; Tok, A. I. Y.; Zhang, Q.; Zhang, H. Fabrication of Single- and Multilayer MoS₂ Film-Based Field-Effect Transistors for Sensing NO at Room Temperature. *Small* **2012**, *8*, 63–67.
- (5) Yin, Z.; Li, H.; Li, H.; Jiang, L.; Shi, Y.; Sun, Y.; Lu, G.; Zhang, Q.; Chen, X.; Zhang, H. Single-Layer MoS₂ Phototransistors. *ACS Nano* **2012**, *6*, 74–80.
- (6) Perkins, F. K.; Friedman, A. L.; Cobas, E.; Campbell, P. M.; Jernigan, G. G.; Jonker, B. T. Chemical Vapor Sensing with Monolayer MoS₂. *Nano Lett.* **2013**, *13*, 668–673.
- (7) Li, H.; Zhang, Q.; Yap, C. C. R.; Tay, B. K.; Edwin, T. H. T.; Olivier, A.; Baillargeat, D.

- 1
2
3 From Bulk to Monolayer MoS₂: Evolution of Raman Scattering. *Adv. Funct. Mater.*
4 **2012**, *22*, 1385–1390.
5
6
7
8
9 (8) Eda, G.; Yamaguchi, H.; Voiry, D.; Fujita, T.; Chen, M.; Chhowalla, M. Photolumines-
10 cence from Chemically Exfoliated MoS₂. *Nano Lett.* **2011**, *11*, 5111–5116.
11
12
13 (9) Splendiani, A.; Sun, L.; Zhang, Y.; Li, T.; Kim, J.; Chim, C.-Y.; Galli, G.; Wang, F.
14 Emerging Photoluminescence in Monolayer MoS₂. *Nano Lett.* **2010**, *10*, 1271–1275.
15
16
17
18 (10) Du, G.; Guo, Z.; Wang, S.; Zeng, R.; Chen, Z.; Liu, H. Superior Stability and High
19 Capacity of Restacked Molybdenum Disulfide as Anode Material for Lithium Ion Bat-
20 teries. *Chem. Commun.* **2010**, *46*, 1106–1108.
21
22
23
24
25 (11) Lopez-Sanchez, O.; Lembke, D.; Kayci, M.; Radenovic, A.; Kis, A. Ultrasensitive Pho-
26 todetectors Based on Monolayer MoS₂. *Nat. Nanotech.* **2013**, *8*, 497–501.
27
28
29
30 (12) Pandey, M.; Vojvodic, A.; Thygesen, K. S.; Jacobsen, K. W. Two-Dimensional Metal
31 Dichalcogenides and Oxides for Hydrogen Evolution: A Computational Screening Ap-
32 proach. *J. Phys. Chem. Lett.* **2015**, *6*, 1577–1585.
33
34
35
36
37 (13) Ataca, C.; Şahin, H.; Ciraci, S. Stable, Single-Layer MX₂ Transition-Metal Oxides and
38 Dichalcogenides in a Honeycomb-Like Structure. *J. Phys. Chem. C* **2012**, *116*, 8983–
39 8999.
40
41
42
43
44 (14) Andersen, A.; Kathmann, S. M.; Lilga, M. A.; Albrecht, K. O.; Hallen, R. T.; Mei, D.
45 First-Principles Characterization of Potassium Intercalation in Hexagonal 2H-MoS₂. *J.*
46 *Phys. Chem. C* **2012**, *116*, 1826–1832.
47
48
49
50
51 (15) X. Qian, L. F., Junwei Liu; Li, J. Quantum Spin Hall Effect in Two-Dimensional Tran-
52 sition Metal Dichalcogenides. *Science* **2014**, *346*, 1344.
53
54
55
56 (16) Voiry, D.; Salehi, M.; Silva, R.; Fujita, T.; Chen, M.; Asefa, T.; Shenoy, V. B.; Eda, G.;

- 1
2
3 Chhowalla, M. Conducting MoS₂ Nanosheets as Catalysts for Hydrogen Evolution Re-
4 action. *Nano Lett.* **2013**, *13*, 6222–6227.
5
6
7
8
9 (17) Lee, Y.-H.; Zhang, X.-Q.; Zhang, W.; Chang, M.-T.; Lin, C.-T.; Chang, K.-D.; Yu, Y.-
10 C.; Wang, J. T.-W.; Chang, C.-S.; Li, L.-J. et al. Synthesis of Large-Area MoS₂ Atomic
11 Layers with Chemical Vapor Deposition. *Adv. Mater.* **2012**, *24*, 2320–2325.
12
13
14
15 (18) Coleman, J. N.; Lotya, M.; O'Neill, A.; Bergin, S. D.; King, P. J.; Khan, U.; Young, K.;
16 Gaucher, A.; De, S.; Smith, R. J. et al. Two-Dimensional Nanosheets Produced by
17 Liquid Exfoliation of Layered Materials. *Science* **2011**, *331*, 568–571.
18
19
20
21
22 (19) Zhou, K.-G.; Mao, N.-N.; Wang, H.-X.; Peng, Y.; Zhang, H.-L. A Mixed-Solvent Strat-
23 egy for Efficient Exfoliation of Inorganic Graphene Analogues. *Angew. Chem. Int. Ed.*
24 **2011**, *50*, 10839–10842.
25
26
27
28
29 (20) Wang, X.; Shen, X.; Wang, Z.; Yu, R.; Chen, L. Atomic-Scale Clarification of Structural
30 Transition of MoS₂ upon Sodium Intercalation. *ACS Nano* **2014**, *8*, 11394–11400.
31
32
33
34 (21) Ou, J. Z.; Chrimes, A. F.; Wang, Y.; Tang, S.-y.; Strano, M. S.; Kalantar-zadeh, K. Ion-
35 Driven Photoluminescence Modulation of Quasi-Two-Dimensional MoS₂ Nanoflakes for
36 Applications in Biological Systems. *Nano Lett.* **2014**, *14*, 857–863.
37
38
39
40
41 (22) Ambrosi, A.; Sofer, Z.; Pumera, M. Lithium Intercalation Compound Dramatically
42 Influences the Electrochemical Properties of Exfoliated MoS₂. *Small* **2015**, *11*, 605–
43 612.
44
45
46
47
48 (23) Wang, Y.; Ou, J. Z.; Balendhran, S.; Chrimes, A. F.; Mortazavi, M.; Yao, D. D.;
49 Field, M. R.; Latham, K.; Bansal, V.; Friend, J. R. et al. Electrochemical Control of
50 Photoluminescence in Two-Dimensional MoS₂ Nanoflakes. *ACS Nano* **2013**, *7*, 10083–
51 10093.
52
53
54
55
56
57
58
59
60

- 1
2
3 (24) Joensen, P.; Frindt, R.; Morrison, S. Single-Layer MoS₂. *Mater. Res. Bull.* **1986**, *21*,
4 457–461.
5
6
7
8 (25) Py, M. A.; Haering, R. R. Structural Destabilization Induced by Lithium Intercalation
9 in MoS₂ and Related Compounds. *Can. J. Phys.* **1983**, *61*, 76–84.
10
11
12 (26) Giannozzi, P.; Baroni, S.; Bonini, N.; Calandra, M.; Car, R.; Cavazzoni, C.; Ceresoli, D.;
13 Chiarotti, G. L.; Cococcioni, M.; Dabo, I. et al. QUANTUM ESPRESSO: A Modular
14 and Open-Source Software Project for Quantum Simulations of Materials. *J. Phys.:
15 Condens. Matter* **2009**, *21*, 395502.
16
17
18 (27) Perdew, J. P.; Chevary, J. A.; Vosko, S. H.; Jackson, K. A.; Pederson, M. R.;
19 Singh, D. J.; Fiolhais, C. Atoms, Molecules, Solids, and Surfaces: Applications of
20 the Generalized Gradient Approximation for Exchange and Correlation. *Phys. Rev. B*
21 **1992**, *46*, 6671–6687.
22
23 (28) Monkhorst, H. J.; Pack, J. D. Special Points for Brillouin-Zone Integrations. *Phys. Rev.*
24 *B* **1976**, *13*, 5188–5192.
25
26 (29) Grimme, S. Semiempirical GGA-Type Density Functional Constructed with a Long-
27 Range Dispersion Correction. *J. Comput. Chem.* **2006**, *27*, 1787–1799.
28
29 (30) Henkelman, G.; Uberuaga, B. P.; Jónsson, H. A Climbing Image Nudged Elastic Band
30 Method for Finding Saddle Points and Minimum Energy Paths. *J. Chem. Phys.* **2000**,
31 *113*, 9901–9904.
32
33 (31) Lin, Y.-C.; Dumcenco, D. O.; Huang, Y.-S.; Suenaga, K. Atomic Mechanism of the
34 Semiconducting-to-Metallic Phase Transition in Single-Layered MoS₂. *Nat. Nanotech.*
35 **2014**, *9*, 391–396.
36
37 (32) Zheng, J.; Zhang, H.; Dong, S.; Liu, Y.; Nai, C. T.; Shin, H. S.; Jeong, H. Y.; Liu, B.;

- 1
2
3 Loh, K. P. High Yield Exfoliation of Two-Dimensional Chalcogenides Using Sodium
4 Naphthalenide. *Nat. comm.* **2014**, *5*.
5
6
7
8
9 (33) Cheng, Y.; Nie, A.; Zhang, Q.; Gan, L.-Y.; Shahbazian-Yassar, R.; Schwingenschlogl, U.
10 Origin of the Phase Transition in Lithiated Molybdenum Disulfide. *ACS Nano* **2014**,
11 *8*, 11447–11453.
12
13
14
15 (34) Wang, Y.; Ou, J. Z.; Chrimes, A. F.; Carey, B. J.; Daeneke, T.; Alsaif, M. M. Y. A.;
16 Mortazavi, M.; Zhuiykov, S.; Medhekar, N.; Bhaskaran, M. et al. Plasmon Resonances
17 of Highly Doped Two-Dimensional MoS₂. *Nano Lett.* **2015**, *15*, 883–890.
18
19
20
21
22 (35) Julien, C. Lithium Intercalated Compounds: Charge Transfer and Related Properties.
23 *Materials Science and Engineering: R: Reports* **2003**, *40*, 47–102.
24
25
26
27 (36) Enyashin, A. N.; Yadgarov, L.; Houben, L.; Popov, I.; Weidenbach, M.; Tenne, R.;
28 Bar-Sadan, M.; Seifert, G. New Route for Stabilization of 1T-WS₂ and MoS₂ Phases.
29 *J. Phys. Chem. C* **2011**, *115*, 24586–24591.
30
31
32
33
34 (37) Mortazavi, M.; Wang, C.; Deng, J.; Shenoy, V. B.; Medhekar, N. V. Ab initio Charac-
35 terization of Layered MoS₂ as Anode for Sodium-ion Batteries. *J. Power Sources* **2014**,
36 *268*, 279–286.
37
38
39
40
41
42
43
44
45
46
47
48
49
50
51
52
53
54
55
56
57
58
59
60

TOC Graphic

